An Iterative Model for Fractal Antennas: Application to the Sierpinski Gasket Antenna

Carles Puente Baliarda, *Member, IEEE*, Carmen Borja Borau, Mònica Navarro Rodero, and
Jordi Romeu Robert, *Member, IEEE*

Abstract—A simple model that explains the behavior of the Sierpinski fractal antenna is presented. This model shows that the multiband behavior of the Sierpinski fractal antenna is a consequence of its fractal nature. The model is applied to predict the behavior of the Sierpinski fractal antenna when the flare angle is modified and its validity is assessed by comparing its predictions with measured data.

Index Terms—Antennas, fractals, multifrequency antennas.

I. INTRODUCTION

THE multiband behavior of the fractal Sierpinski dipole has been presented and discussed in [1]–[3]. The analysis and results showed that the antenna had a log-periodic behavior, the log-period being related to the self-similarity scale factor of the antenna.

The current distribution on the Sierpinski gasket shows that the most of the current density concentrates on the joints and edges of the different triangle clusters that make up the Sierpinski gasket [3]. This fact suggested a very simple iterative transmission line model for the Sierpinski antenna that will be discussed in Section II. This simple model based on the iterative transmission line model has already been successfully applied to predict the behavior of the Sierpinski microstrip network [4], and it shows that the multiband properties of the Sierpinski gasket are inherent to its fractal structure. The validity of the model is assessed by applying the iterative transmission line model to three fractal Sierpinski antennas with flare angles of $\alpha = 30°$, $\alpha = 60°$, and $\alpha = 90°$. The measured results are in good agreement with the predictions made by the model. On the other hand, as suggested by [5] it is possible to modify the input impedance of triangular antennas such as the bow-tie antenna by changing the flare angle of the antenna. A similar conclusion is reached for the Sierpinski antenna. In Section III the patterns and the current distributions of the Sierpinski antenna for different flare angles are presented. The patterns and the current distribution help to understand some of the limitations of this kind of antennas.
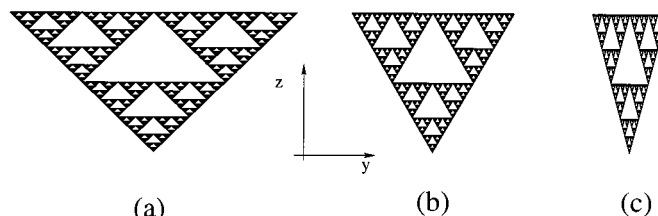
Fig. 1. Sierpinski gaskets with different flare angle: (a) $\alpha = 90°$, (b) $\alpha = 60°$, (c) $\alpha = 30°$.

II. ITERATIVE TRANSMISSION LINE MODEL

The way the Sierpinski gasket is built can be understood as an iterative feed-back process, where a set of similarity transformations are iteratively applied to an initiator [6]. For the Sierpinski gasket three similarity transformations are required, each one of them consists on a reduction by a scale factor of 0.5 and a translation. The very same process employed in the construction of the Sierpinski gasket is used in the definition of the iterative transmission line model. As initiator a three port network is considered. It is assumed that the initiator of the Sierpinski gasket is an isosceles triangle; consequently, due to the symmetry and reciprocity properties of the initiator the $[S]$ matrix has the following structure:

$$[S] = \begin{bmatrix} \alpha & \beta & \beta \\ \beta & \gamma & \delta \\ \beta & \delta & \gamma \end{bmatrix} \tag{1}$$

that is, four parameters are necessary to fully describe the network. Given one iteration the next one is built as shown in [4]. After a simple, but rather lengthy analysis it can be shown that the corresponding parameters of the next iteration $[S_{n+1}]$ can be written as

$$\alpha_{n+1} = \alpha_n + 2\beta_n^2 \left(\alpha_n + \frac{\beta_n^2}{1-\gamma_n} \right)$$
$$\cdot \frac{1}{1 - (\gamma_n + \delta_n)\left(\alpha_n + \frac{\beta_n^2}{1-\gamma_n} \right)} \tag{2}$$

$$\beta_{n+1} = \left(1 + \frac{\delta_n}{1-\gamma_n} \right) \frac{\beta_n^2}{1 - (\gamma_n + \delta_n)\left(\alpha_n + \frac{\beta_n^2}{1-\gamma_n} \right)} \tag{3}$$

$$\gamma_{n+1} = \gamma_n + \frac{\beta_n(E_nH_n + G_n) + \delta_n(G_nB_n + H_n)}{1 - B_nE_n} \tag{4}$$
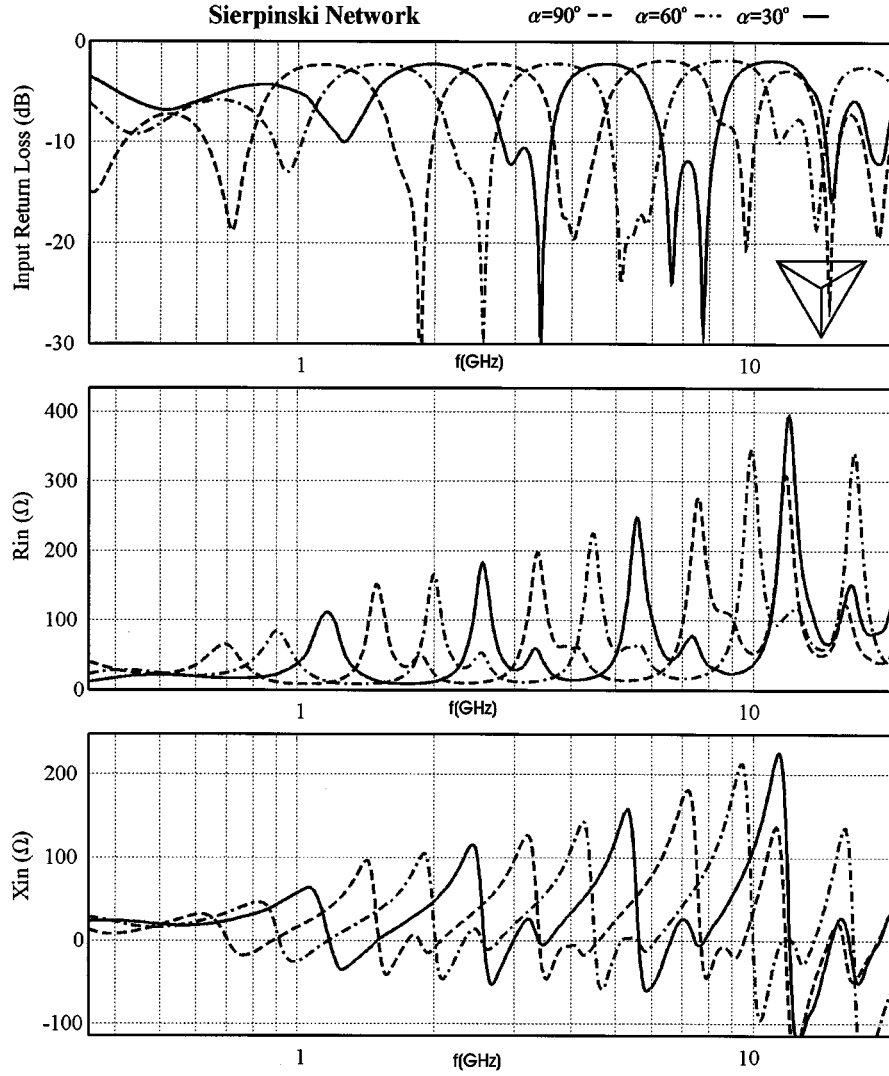
Fig. 2.   Input impedance for the Sierpinski gasket antenna according to the transmission line iterative model.

$$\delta_{n+1} = \frac{\beta_n(E_n C_n + F_n) + \delta_n(B_n F_n + C_n)}{1 - B_n E_n} \qquad (5)$$

where the auxiliary parameters B, C, E, F, G, H are defined as

$$B = \left(\gamma + \frac{\delta\alpha + \gamma\beta^2}{1 - \alpha\gamma}\right) \frac{\beta}{1 - \gamma^2 - \frac{\beta^2(\delta + \gamma^2)}{1 - \alpha\gamma}} \qquad (6)$$

$$C = \frac{\left(\delta + \frac{\beta^2\gamma}{1 - \alpha\gamma}\right)}{1 - \gamma^2 - \frac{\beta^2(\delta + \gamma^2)}{1 - \alpha\gamma}} \qquad (7)$$

$$E = \beta \frac{\gamma + \frac{\delta(\delta\alpha + \gamma)}{1 - \alpha\gamma}}{1 - \alpha\gamma - \frac{\delta(\delta\alpha^2 + \beta^2)}{1 - \alpha\gamma}} \qquad (8)$$

$$F = \frac{\frac{\beta\delta}{1 - \alpha\gamma}}{1 - \alpha\gamma - \frac{\delta(\delta\alpha^2 + \beta^2)}{1 - \alpha\gamma}} \qquad (9)$$

$$G = \frac{\beta\gamma + (1 + \alpha)\frac{\beta\delta^2}{1 - \alpha\gamma}}{1 - \alpha\gamma - \frac{\delta(\delta\alpha^2 + \beta^2)}{1 - \alpha\gamma}} \qquad (10)$$

$$H = \frac{\delta\gamma + (1 + \gamma)\frac{\beta^2\delta}{1 - \alpha\gamma}}{1 - \gamma^2 - \frac{\beta^2(\delta + \gamma^2)}{1 - \alpha\gamma}} \qquad (11)$$
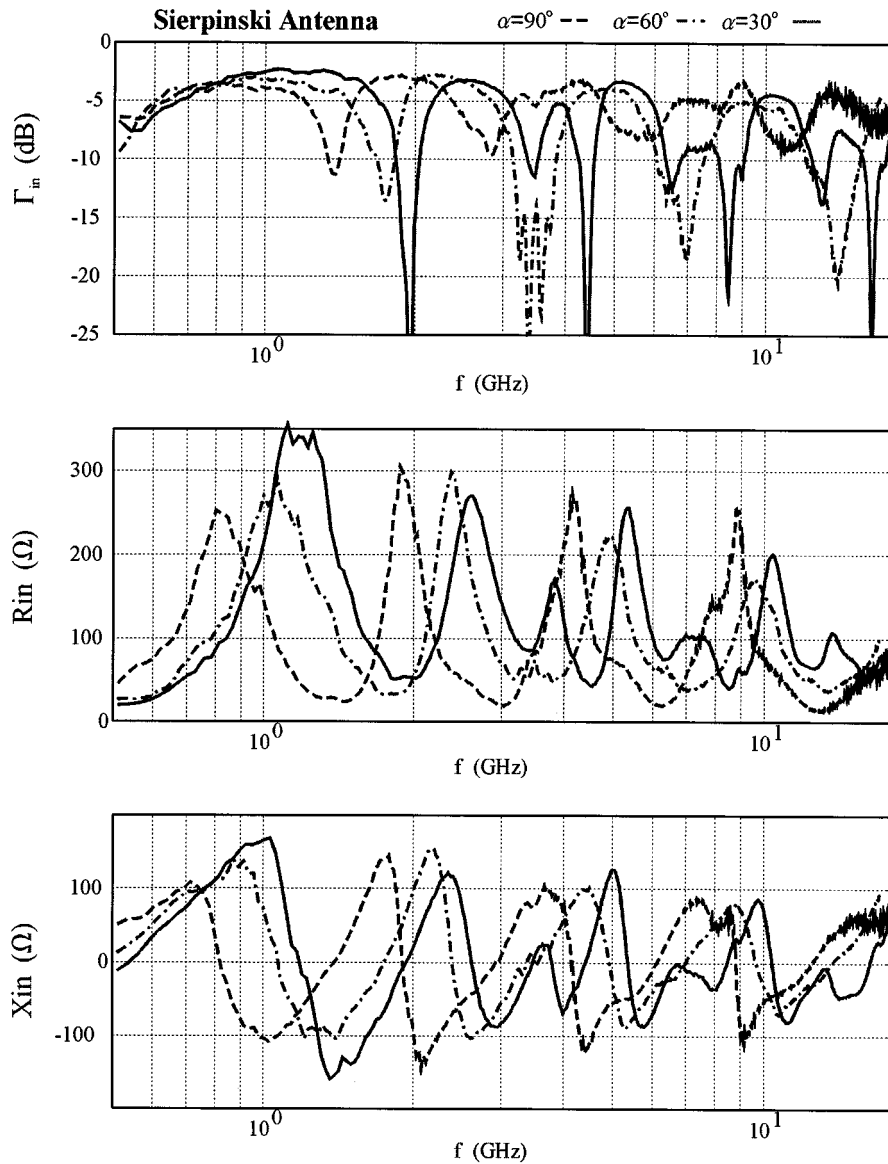
Fig. 3. Measured input impedance for the Sierpinski gasket antenna for $\alpha = 30°$, $\alpha = 60°$, $\alpha = 90°$.

The input reflection coefficient Γ_{in} of the three port network when ports 2 and 3 are loaded by Γ_2 and Γ_3, respectively, is given by

$$\Gamma_{\text{in}} = \alpha + \frac{\beta^2}{D1}\Gamma_2\left(1 + \frac{\delta\Gamma_3}{1 - \gamma\Gamma_3}\right)$$
$$+ \frac{\beta^2}{D2}\Gamma_3\left(1 + \frac{\delta\Gamma_2}{1 - \gamma\Gamma_2}\right) \tag{12}$$

where, again, the auxiliary parameters $D1$ and $D2$ are defined as

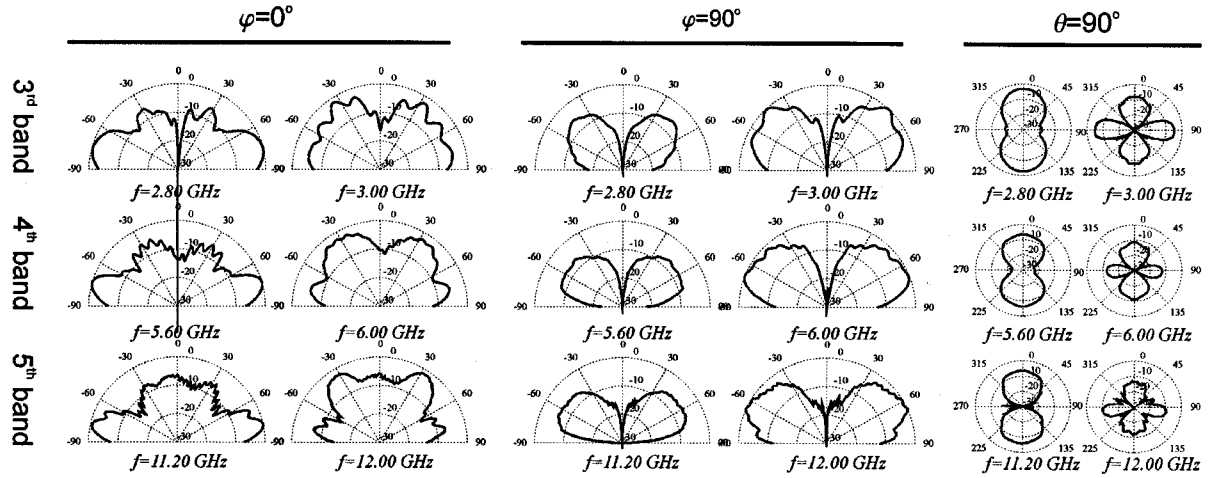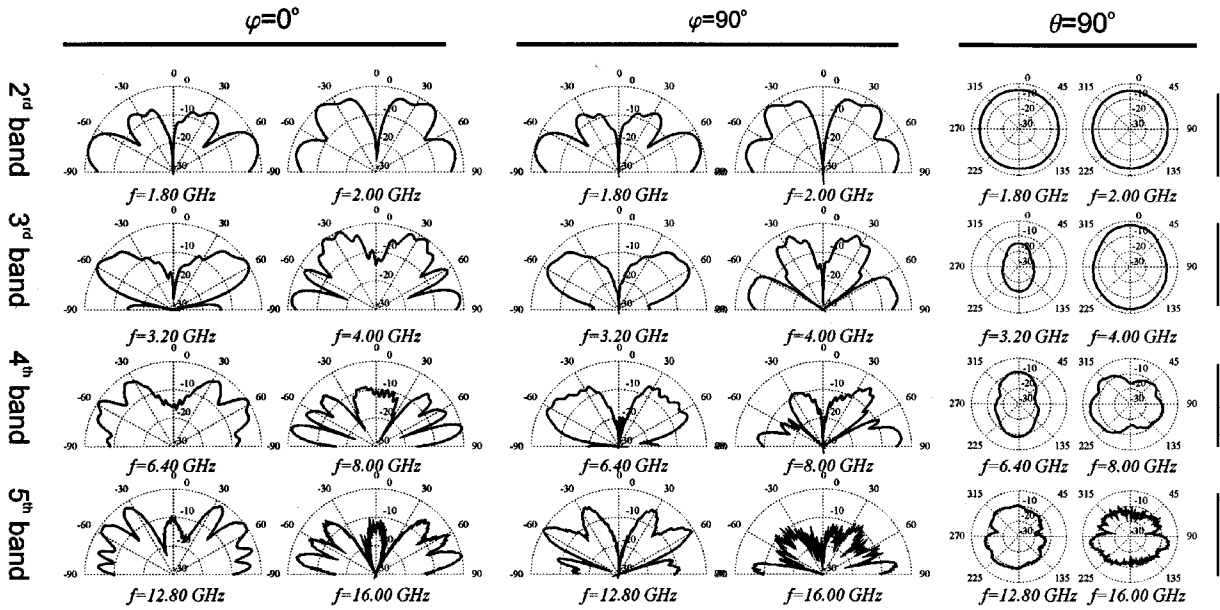$$D1 = 1 - \gamma\Gamma_2 - \frac{\delta^2\Gamma_2\Gamma_3}{1 - \gamma\Gamma_3} \tag{13}$$

$$D2 = 1 - \gamma\Gamma_3 - \frac{\delta^2\Gamma_2\Gamma_3}{1 - \gamma\Gamma_2}. \tag{14}$$

For the equilateral Sierpinski, that is, flare angle $\alpha = 60°$, additional symmetry relations can be found and the $[S]$ matrix can be written as

$$[S] = \begin{bmatrix} \alpha & \beta & \beta \\ \beta & \alpha & \beta \\ \beta & \beta & \alpha \end{bmatrix}. \tag{15}$$

The recursion relations of (2)–(5) simplify to

$$\alpha_{n+1} = \alpha_n + \frac{2\beta_n^2\left(\alpha_n + \frac{\beta_n^2}{1 - \alpha_n}\right)}{1 - (\alpha_n + \beta_n)\left(\alpha_n + \frac{\beta_n^2}{1 - \alpha_n}\right)} \tag{16}$$

Fig. 4. Radiation pattern for the $90°$ Sierpinski monopole.

Fig. 5. Radiation pattern for the $30°$ Sierpinski monopole.

$$\beta_{n+1} = \frac{\beta_n^2 \left(1 + \dfrac{\beta_n}{1 - \alpha_n}\right)}{1 - (\alpha_n + \beta_n)\left(\alpha_n + \dfrac{\beta_n^2}{1 - \alpha_n}\right)}. \tag{17}$$

This very simple recursive model allows to predict the behavior of the input parameters of the Sierpinski antenna for any iteration stage. Any symmetrical, reciprocal three-port network able to store electric and magnetic energy could be used to model the initiator. For the following results a symmetrical Y junction of lossy lines has been considered. The length of

the transmission lines is simply determined by the height of the whole gasket, the number of iterations, and the flare angle. In order to account for the radiation losses a finite Q factor has been considered by introducing an attenuation factor in the transmission lines. The characteristic impedance of the transmission lines of the three-port equivalent circuit has been empirically adjusted to $5Z_0$, where Z_0 is the reference impedance.

This model does not make a good prediction of the antenna impedance at low frequencies, that is, below the first resonance. The accuracy of the model can be improved if the ports 2 and 3 of the complete Sierpinski network are loaded to take into account the radiation resistance at low frequencies, that appears to be underestimated by the lossy transmission model. To take
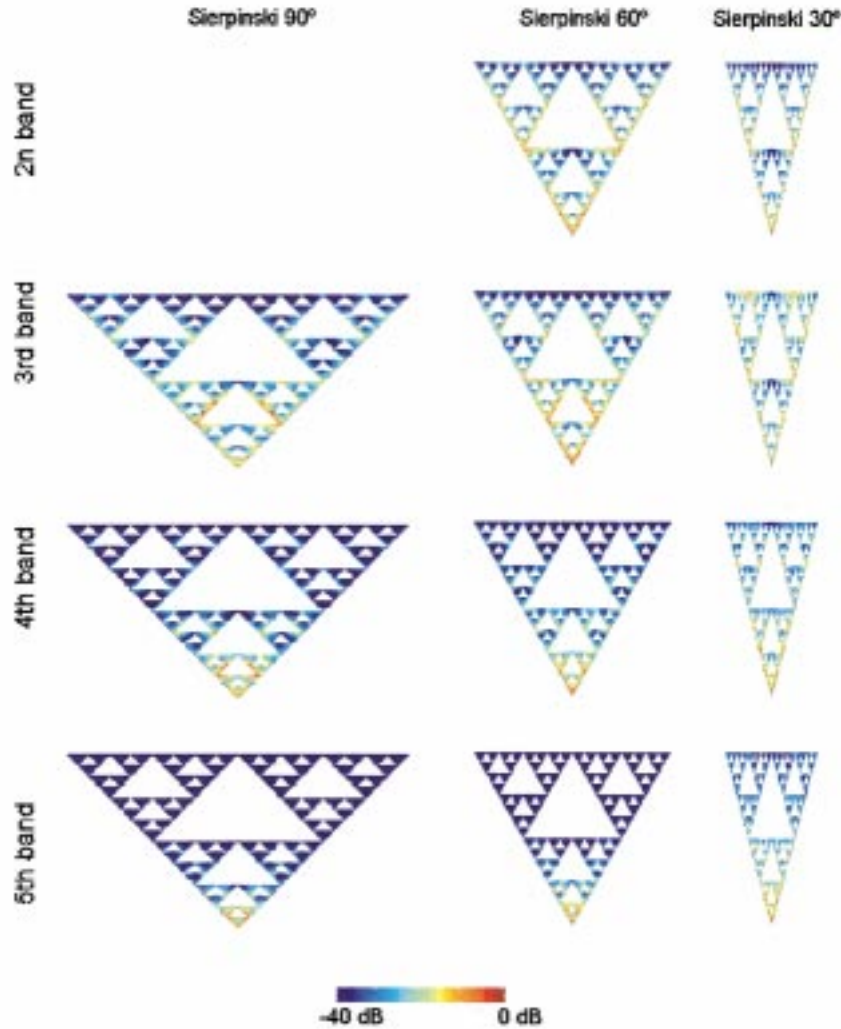
Fig. 6. Current distribution on the antennas.

into account this effect a frequency dependent resistive load of the form

$$R_L \propto \left(\frac{h}{c} f\right)^2 \qquad (18)$$

has been chosen, where h is the height of the antenna. The parabolic dependence as a function of the frequency takes into account the radiation resistance behavior of a small antenna. At higher frequencies the effect of the terminating load is neglectable for two reasons. First, as the frequency increases the load tends to be an open circuit, and second due to the radiation losses of the antenna the current does not reach the tips of the antenna; consequently, at high frequencies, the value of the terminating load is irrelevant.

Three Sierpinski gaskets, as shown in Fig. 1, with flare angles of $\alpha = 90°$, $\alpha = 60°$, and $\alpha = 30°$, were built and tested. The antennas were measured in a monopole configuration over an 80×80 cm ground plane. The antennas were etched on CuClad 250 dielectric substrate ($\epsilon_r = 2.5$, width $= 1.588$ mm), and the height for the three antennas was 8.9 cm. The input reflection coefficient was measured relative to $50\ \Omega$. Fig. 2 shows the result for the iterative transmission line model, and Fig. 3 shows the measured results. The log-periodic behavior of the antennas is clearly evinced when the resonant frequency at each band is considered. Except for the first band, the resonant frequencies for the monopole Sierpinski antenna can be computed as

$$f_r = 0.152 \frac{c}{h} \cos(\alpha/2)(\delta)^n \qquad (19)$$

where

c speed of light;
h height of the monopole;
α flare angle;
δ log-period (two in this case);
n band number.

The first band is referred as the bowtie mode of the antenna. At the first resonance, the truncation effect is clearly dominant in the Sierpinski antenna and the etched holes are not significant due to their size compared to the wavelength as reported in [3]. Equation (19), clearly evinces two important facts about the Sierpinski gasket antenna, the log-periodic behavior, and that

the resonant frequencies are associated to the gasket edge length rather than to its height.

The iterative transmission line model provides a good prediction of the behavior of the Sierpinski antenna. The number of resonant frequencies is correctly predicted and it is also shown that as the flare angle increases the resonant frequencies move to lower frequencies. As the height of the antenna is the same for the three cases, the increase of the flare angle implies longer edges of the triangles. The fact that the transmission line model correctly predicts the frequency down shifting corroborates the assumption that the current distribution on the antenna is basically supported on the edges. The iterative transmission line model does not assume any mutual effects between different antenna clusters, however, the model is accurate enough the predict the overall behavior of the antenna. It even predicts the double resonances that appear for $\alpha = 30°$ in the upper three bands. The significance of these double resonances will be discussed in the following section. The major differences appear in the prediction of the impedance at the anti-resonant frequencies. Finally, it is important to notice that the multiband properties of the antenna stem from the iterative way it is constructed and that has been replicated by the iterative transmission line model.

III. RADIATION PATTERNS

The measured radiation patterns of the fractal Sierpinski monopoles are presented in Figs. 4 and 5 for the flare angles of $\alpha = 90°$ and $\alpha = 30°$, respectively. The pattern corresponding to the bowtie mode, that is, the first band is omitted. The patterns corresponding to $\alpha = 60°$ can be found in [3] and are not reproduced here. The patterns show the θ component of the radiated field. Two frequencies have been measured at each band. For the case $\alpha = 90°$ the lower band has not been measured as it is below the capabilities of the antenna range. The patterns for $\alpha = 90°$ exhibit some characteristics already found for $\alpha = 60°$. The pattern has a log-periodic behavior, that is the same pattern is found when the frequency is multiplied by a factor of 2. On the other hand, the pattern changes within the same band, therefore, it is not a frequency independent antenna. The patterns for $\alpha = 30°$ exhibit a different behavior. As the frequency increases the pattern has an increasing number of lobes. This behavior resembles more that of a linear monopole than the multiband behavior of the fractal antenna. A better understanding of the behavior of the antenna can be gained from the current distribution.

The current distribution of the three antennas has been computed by means of the FDTD method. The total current distribution is shown in Fig. 6. For the cases in which $\alpha = 60°$ and $\alpha = 90°$ the current distribution has a similar pattern from band to band, except for a scale factor. The antennas have an active region whose size reduces by a factor of two every time the frequency is increased by a factor of two. On the contrary, in the case $\alpha = 30°$ the current distribution is not confined to an active region but it is distributed along the whole geometry of the antenna.

The explanation has to be found in the shorter length of the edges of the triangular clusters for $\alpha = 30°$. In this case, the antenna becomes a poor radiator and the current distribution is not confined to an active region but it reaches the end of the antenna. This fact was already anticipated by the input parameters of the antenna. The fact that for $\alpha = 30°$ double resonances were predicted by the iterative transmission line model and actually measured, suggests a double mode of operation of this antenna. One of them is what can be called the Sierpinski mode associated with the first resonance of the corresponding scale of the fractal. The second mode corresponds to harmonic resonances of the larger scales of the fractal. The superposition of both modes causes the current distribution on the antenna to extend to the whole structure. The result is seen in the radiation patterns of the antenna. The proper interpretation of this result shows that the Sierpinski fractal antenna can be interpreted as a succession of resonators embedded in each other. In this case each resonator has a reduction in scale of two, therefore, the fundamental resonant frequency doubles for each resonator. For large flare angles just the fundamental resonant mode of one resonator is excited, but for smaller flare angles and due to the smaller radiation losses harmonic modes of the larger resonators are also excited. Similar limitation should be expected in fractal structures in which poor radiation resistance of the individual clusters would lead to a masking of the log-periodic behavior by the existence of harmonic resonances in the structure.

IV. CONCLUSION

The iterative transmission line model is a very simple approach that models the Sierpinski fractal antenna by following the same iterative process that is employed in the construction of the Sierpinski gasket. The model gives a good prediction on the behavior of the antenna including some second-order effects as the ones discussed for the antenna with $\alpha = 30°$. The model also shows that the log-period nature of the antenna is inherent to its fractal structure that is somehow replicated by the iterative transmission line model. It has also been highlighted that a self-similar structure has by its very own nature a log-periodic behavior, but this behavior can be masked in certain cases by the presence of harmonic resonances in the structure.

REFERENCES

[1] C. Puente, "Fractal Antennas," Ph.D dissertation, Dept. Signal Theory Commun./Univ. Politecnica de Catalunya, Spain, June 1997.
[2] C. Puente, J. Romeu, R. Pous, X. Garcia, and F. Benitez, "Fractal multiband antenna based on the Sierpinski gasket," *Electron. Lett.*, vol. 32, no. 1, pp. 1–2, Jan. 1996.
[3] C. Puente, J. Romeu, R. Pous, and A. Cardama, "On the behavior of the Sierpinski multiband antenna," *IEEE Trans. Antennas Propagat.*, vol. 46, pp. 517–524, Apr. 1998.
[4] C. Borja, C. Puente, and A. Medina, "Iterative network model to predict the behavior of a Sierpinski fractal network," *Electron. Lett.*, vol. 34, no. 15, pp. 1443–1445, July 23, 1998.
[5] G. H. Brown and O. M. Woodward, "Experimentally determined radiation characteristics of conical and triangular antennas," *RCA Rev.*, pp. 425–452, Dec. 1952.
[6] H. O. Peitgen, H. Jurgens, and D. Saupe, *Chaos and Fractals, New Frontiers in Science*. New York: Springer-Verlag, 1992.

Carles Puente Baliarda (S'91–M'93) was born in Badalona, Spain, in 1968. He received the Ing. degree in telecommunications engineering from the Polytechnic University of Catalonia (UPC), Barcelona, Spain, in 1992, the M.S. degree from the University of Illinois at Urbana-Champaign (UIUC), in 1994, and the Ph.D. degree from the UPC, in 1997.

From 1994 to 1999, he joined the faculty of the Electromagnetics and Photonics Engineering Group (EEF), UPC, and worked there in LIDAR systems and in the development of the fractal technology applied to antennas and microwave devices. He is one of the founders of Fractus S.A. and, since September 1999, he has held the Technology Director position there. He holds several patents on fractal and other related antenna and microwave inventions.

Dr. Puente Baliarda received the Best Doctoral Thesis Award in Mobile Communications in 1997 by the Colegio Oficial de Ingenieros de Telecomunicación (COIT) and ERICSSON and, in 1998, he and his team received the European Information Technology Grand Prize from the European Council for the Applied Science an Engineering (EuroCASE) and the European Comission for his work in fractal-shaped antennas and their application to cellular telephony.

Carmen Borja Borau was born in Barcelona, Spain, in 1972. She received the Ing. degree in telecommunications engineering from the Polytechnic University of Catalonia, Barcelona, Spain, in 1997. She is currently working toward the Ph.D. degree at the Polytechnic University of Catalonia, Spain.

Since 1997, she has been on a Scholarship at the Department of Signal Theory and Communications (TSC), Polytechnic University of Catalonia. Her research interests are fractal and microstrip antennas.

Mònica Navarro Rodero was born in Barcelona, Spain, in 1973. She received the Ing. degree in telecommunications engineering from the Universitat Politecnica de Catalunya (UPC), Barcelona, Spain, in 1997.

In 1997, she joined the Department of Signal Theory and Communications, UPC, as a Postgraduate student where she has been granted a scholarship. Her main research interest is multiband fractal antennas.

Jordi Romeu Robert (S'88–M'93) was born in Barcelona, Spain, in 1962. He received the Ing. and Doctor Ing. degrees in telecommunication engineering, both from the Polytechnic University of Catalonia (UPC), Barcelona, Spain, in 1986 and 1991, respectively.

In 1985, he joined the Electromagetic and Photonic Enginnering Group of the Signal Theory and Communications Department, UPC. Currently, he is Associate Professor there and is engaged in research in antenna near-field measurments, antenna dignostics, and antenna design. He was Visiting Scholar at the Antenna Laboratory, University of California, Los Angeles, in 1999.